

A Model-based Dynamic Toll Pricing Strategy
for Controlling Highway Traffic

by

Thao Kim Phan

B.S. in Mechanical Engineering
Massachusetts Institute of Technology, 2013

Submitted to the Department of Mechanical Engineering
in partial fulfillment of the requirements for the degree of

Master of Science in Mechanical Engineering

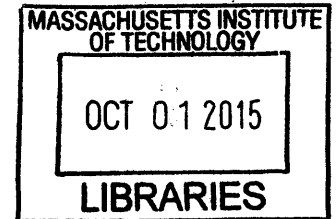
at the

MASSACHUSETTS INSTITUTE OF TECHNOLOGY

September 2015

© 2015 Massachusetts Institute of Technology. All rights reserved.

ARCHIVES



Signature of Author _____ **Signature redacted** _____

Department of Mechanical Engineering
August 20, 2015

Certified by _____ **Signature redacted** _____

Dr. ~~Aniradha~~ Annaswamy
Senior Research Scientist
Thesis Supervisor

Accepted by _____ **Signature redacted** _____

David E. Hardt
Chairman, Department Committee on Graduate Students

A Model-based Dynamic Toll Pricing Strategy for Controlling Highway Traffic

by

Thao Kim Phan

Submitted to the Department of Mechanical Engineering
on August 20, 2015, in partial fulfillment of the
requirements for the degree of
Master of Science in Mechanical Engineering

Abstract

A model-based approach to dynamic toll pricing has been developed to provide a systematic method for determining optimal freeway pricing schemes. A novel approach is suggested for alleviating traffic congestion, which utilizes identified models of driver behavior and traffic flow, as well as optimization of the target density to maximize throughput. Real-time traffic information from on-road sensors is integrated with historical information to provide feedback and preview for the dynamic toll price controller. The algorithm developed here provides an opportunity to improve on existing toll policy by guaranteeing minimum speeds for toll lane drivers, maintaining consistent traffic flow for the other drivers, and optimizing the overall traffic throughput.

Thesis Supervisor: Dr. Anuradha Annaswamy
Title: Senior Research Scientist

Acknowledgements

Firstly, I would like to thank my advisor Dr. Annaswamy for giving me the opportunity to work on this project. The knowledge, experience, and guidance you've provided me has made me a better researcher.

I would also like to acknowledge my colleagues at the Ford Motor Company, Diana Yanakiev and Eric Tseng, for their continuous support and for giving me the opportunity to work alongside them in the summer of 2014. Diana's mentorship and Eric's expertise and insight have undoubtedly improved my work and skills as an engineer.

Also, I would like to acknowledge Mike Solomonson and Brian Kary at MnDOT for providing MnPASS data and information on the MnPASS dynamic toll pricing system. Their contributions to this thesis are invaluable.

Finally, I would like to thank my family and friends for their support.

This work was supported by the Ford-MIT Alliance.

Contents

1	Introduction	10
1.1	Problem Motivation	10
1.2	Thesis Outline	11
2	Background	12
2.1	Toll Pricing	12
2.2	Dynamic Toll Pricing Today	13
2.3	Literature Review	15
2.3.1	Traffic Flow Theory	15
2.3.2	Dynamic Pricing Research	17
3	Socio-Technical Model	18
3.1	Traffic Flow Model	19
3.1.1	Traffic Flow Dynamics	19
3.1.2	Traffic Flow Dynamics Parameterization	20
3.2	Traffic Equilibrium	20
3.2.1	Equilibrium Model and Parameterization	20
3.3	Alternative Traffic Models	22
3.4	Driver Behavior Model	23
3.4.1	Logit Model	23
3.4.2	Driver Behavior Parameterization and Recursive Least Squares Estimation	24
4	Model-Based Price Control Strategy	27
4.1	PD Controller	28
4.2	Feedforward Controller	28

4.3	Inverse Driver Behavior Component	29
4.4	Gain Tuning	29
4.5	Results	30
4.5.1	Model Validation	30
4.5.2	Results of our Model-based Pricing Controller	31
4.5.3	Effect of the Inverse Driver Behavior Component	33
4.5.4	Target Density Selection	34
4.5.5	Revenue Effects	35
4.5.6	MATSIM	35
5	Conclusion and Future Work	38
5.1	Contributions of this Thesis	38
5.2	Discussion of Future Work	39
A	MATLAB/Simulink	43
A.1	Parameterization	43
A.2	Simulink	46

List of Figures

2.1	The optimum toll price based on economic analysis.	13
2.2	A map of the operations of MnPASS on I-35.	13
2.3	The loop detector used for road measurements.	14
2.4	A table of the MnPASS pricing system. Here K represents the density. A default rate is chosen based what level of service the maximum density falls in and is adjusted based on the change in density. Minimum and maximum values o	15
3.1	A physical schematic of the road segment. The HOT lane is in parallel with the GPL. No traffic flows between the two beyond are assumed to occur the initial entry point.	18
3.2	A higher-level block diagram for our dynamic pricing system. The price influences the number of drivers that go into each lane, which is determined by the driver behavior model. The number of vehicles, then, affect the lane densities, closing the loop.	19
3.3	The physical map of the road segment (3.3a) and the schematic (3.3b). The road segment chosen lies on I-35W. Black dots on 3.3a indicate sensor locations. Figure 3.3b reveals operational details concerning the location of toll collection, restricted entrances, and toll rate signs. . .	21
3.4	The equilibrium relationship between speed and density.	22
3.5	A hysteresis curve in the congested region of traffic.	23
3.6	The logistic model used to characterize driver behavior and determine the HOT usage. The input to the model is the driver utility, which is a weighted sum of the current toll price and perceived time savings. .	25

4.1	The inputs, subsystems, and variables of the entire system are shown in this representative block diagram. The input into the system is the desired density in the HOT lane, and the output is the actual density. The input flow is the measured, total flow into the system.	27
4.2	The MnPASS pricing controller was placed alongside our socio-technical model to validate the use of our system model.	30
4.3	The similarity of the density and speed plots of our simulated system (blue) and the actual MnPASS system (red) validate the use of our model-based system.	31
4.4	PID gains were chosen in 4.4a to match the behavior of MnPASS (red) and validate our system model (blue). The gains were changed for the simulation run in 4.4b to yield a more aggressive pricing scheme that was successful in preventing congestion in the HOT lane.	32
4.5	High input flow is introduced in the middle of the operating period to test the systems' ability to prevent congestion. The model-based system is successful in keeping the HOT density low compared to MnPASS.	33
4.6	While the system without the inverse driver behavior pricing component (right) is able to keep the system from experience congestion, it fluctuates about the target density much more than the system with the inverse behavior component (left).	34
4.7	Increasing the reference density can increase the overall segment flow to maximize throughput.	35
4.8	With an aggressive choice for the pricing controller, revenue can increase while maintaining the speed advantage in the HOT lane. . . .	36
4.9	Testing our pricing controller in MATSIM.	36
4.10	Testing our pricing controller in MATSIM.	37

List of Tables

3.1	Mean values of fitted driver behavior parameters by day of the week .	26
4.1	K_d values	30

Chapter 1

Introduction

1.1 Problem Motivation

Traffic congestion is daily headache and source of stress for the average commuter. Consider the increasing growth of urban areas in the last few decades and, along with it, the overwhelming number of vehicles on the road, and the problem of traffic congestion becomes a vital issue that needs to be addressed. Over one billion cars travel on the roads today, and that number is projected to double by 2020 [16]. Many efforts to reduce congestion involve investing into public transportation to lower the number of cars on the roads, but it is understood that these operations generally require years of planning, significant funds, and an underlying city geography conducive to public transit. Even increasing the number of lanes on highways can be ineffective in alleviating the problem of rising traffic congestion, as it has been seen that that addition comes with a corresponding rise in highway drivers. Unfortunately, driving a car is an unavoidable choice for at least 65% of city populations, who rely on their vehicles to get to school or work [14], so efforts to solve the problem of traffic congestion must also address the unavoidable fact that people will continue to use and buy cars.

The problem with traffic congestion is, for those commuters who are forced to drive through these rush hours daily, the lost time can be a significant cost when considered over a lifetime. For example, traveling in New York City takes 50-75% longer during peak hours. When translated into a monetary cost, traffic congestion in NYC causes a loss of \$8 billion a year. As reported in [9], the number of hours spent in traffic jams over a five day period, for the cities in France, Honolulu, San Francisco, and Los Angeles are 35, 56, 60, and 64, respectively. For an individual driver, each

hour in traffic costs about \$21 [9]. In addition to these time-related costs, the mental aspect of driving in traffic should not be ignored. A global study by IBM revealed that 55% of those surveyed incurred 30-60 minutes of delay due to traffic jams, with 42% reporting increased stress levels [14]. The IBM survey also indicated that 41% believe the problem of traffic is getting worse, despite the efforts of transportation officials and city planners.

New solutions are needed to fix the problem of traffic congestion. Within the last few years, intelligent transportation systems have been introduced and implemented, especially in the United States. For example, real-time traffic information from cell-phone signals is being used by Google Maps to give its users travel time predictions and suggested routes. Smartphone applications like Waze now have the capability of providing reports of the current state of traffic based on user submissions. Through the works of local transportation departments, posted signs on highways also offer estimated travel times. For decades, toll pricing has been utilized as a form of congestion pricing, and within the last decade, a new form of toll pricing, one which charges a dynamic toll based on real-time traffic conditions, has been employed to manage traffic congestion. The focus of this thesis is a novel dynamic toll pricing scheme that alleviates congestion and maintains desired traffic conditions during peak hour times.

1.2 Thesis Outline

The remainder of this thesis is as follows. Chapter 2 provides a comprehensive background of toll pricing in the United States and a literature review of research in the area of dynamic toll pricing. Chapter 3 describes the socio-technical model that has been developed to describe driver behavior and traffic flow. The parameterization of the models are also given in this chapter. The details of the dynamic pricing controller are explained in Chapter 4, along with the results. Finally, Chapter 5 closes with concluding remarks and directions for future work.

Chapter 2

Background

2.1 Toll Pricing

Charging drivers for passage on a road has been around since the 1970's, and academic interest in the area has been around even earlier than that. In the 1950's, William Vickrey, an economist, wrote on the necessity of road pricing for NYC. Consider highway traffic in the context of classical economics, where demand curve denotes the demand by drivers for use of the highway and traditional supply curve represents the individual cost of travel (purple line in Fig. 2.1) [23]. For an untolled highway, because individual drivers do not suffer the cost of congestion that they impose on other drivers (a negative externality), a toll ($\$P^* - P^0$) must be charged in order for the drivers to experience the actual total costs (orange in Fig. 2.1), resulting in demand volume lowering to bring the road system into an equilibrium, which yields a highway without congestion [24].

Due to rising congestion, the first country to impose a road toll was Singapore in 1975, and they continued to innovate in this area by introducing the first electronic toll collection in 1998 [10]. Toll pricing is currently implemented in most of the major cities in the world and can, indeed, result in reductions of road traffic. However, car ownership and city populations continue to grow and outpace the development of new roads, and many of these metropolitans do not have the space to expand their existing roads. Traffic congestion is still a major problem that needs to be addressed beyond these basic principles, and dynamic toll pricing is suggested in this thesis as a solution to the problem.

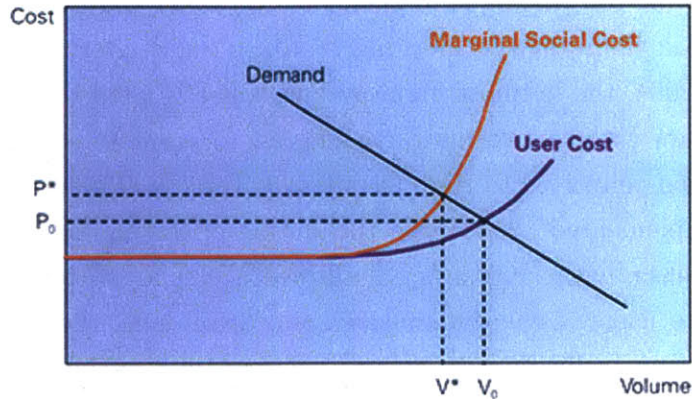


Figure 2.1: The optimum toll price based on economic analysis.

2.2 Dynamic Toll Pricing Today

A different type of toll pricing has arisen in the past few years, one which reacts to the real-time, measured traffic conditions, which is in contrast to a static pricing system, which has a fixed toll price at a set time period. Dynamic toll pricing systems have gained popularity within the last decade, especially in the United States. The addition of sensors on the roads allows transportation authorities to know the traffic conditions at every minute, and naturally, toll pricing systems based on these sensor measurements have been implemented. The earliest dynamic toll pricing system in the US originated in 2004 in Minneapolis, MN [8], termed MnPASS, and many other cities have followed suit and also adopted dynamic toll pricing. These systems can be seen in Seattle, WA, Dallas, TX, Atlanta, GA, Los Angeles, CA, and Virginia [1, 3, 4, 25]. The toll pricing strategy proposed in this paper is designed, analyzed, and evaluated using the MnPASS traffic data.

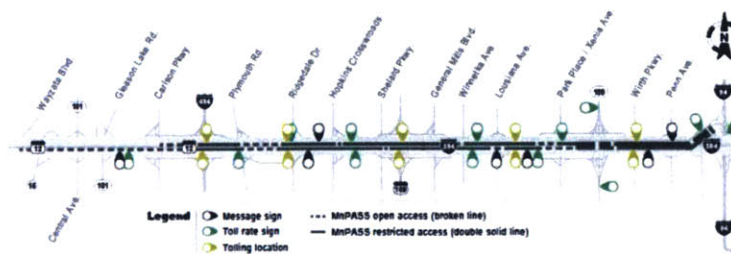


Figure 2.2: A map of the operations of MnPASS on I-35.

Currently, dynamic toll pricing is implemented on I-394 and I-35 in Minneapolis, MN during the peak hours in the morning (6-10AM) and afternoon (3-7PM) (see Fig. 2.2). Prior to 2004, the leftmost highway lane was allocated to High Occupancy Vehicles (HOV), cars with two or more passengers, to promote carpool use. These HOV lanes were then converted to High Occupancy Toll (HOT) lanes when dynamic toll pricing was implemented, charging a toll during operating hours and reverting to free lanes otherwise, with HOV's being allowed access at no toll. To determine the price charged to users of the dynamically priced toll lane, the MnPASS system collects data regarding traffic speeds, v , and volumes, in real-time, using inductive loop detectors embedded into the roads (see Fig 2.3). The free lanes are referred to as general purpose lanes (GPL). The MnPASS system, then, estimates the densities at each of the sensor locations based on Eqs. (2.1-2.3). Measurements of occupancy (the time it takes for a vehicle to travel from one edge of the sensor to the other edge), $o(t)$, and volume (the number of cars that pass the sensor), $V(t)$, are collected over a sampling period, T_s , of thirty seconds. With the sensor field length, L_{sensor} , and the sampling time of the sensor known, speed, v , and flow, q , data can be derived from occupancy and volume, respectively. Local density, ρ , at the sensors can then be obtained by,

$$v = \frac{L_{sensor}}{o(t)} \quad (2.1)$$

$$q = \frac{V(t)}{T_s} \quad (2.2)$$

$$\rho = \frac{v}{q}. \quad (2.3)$$

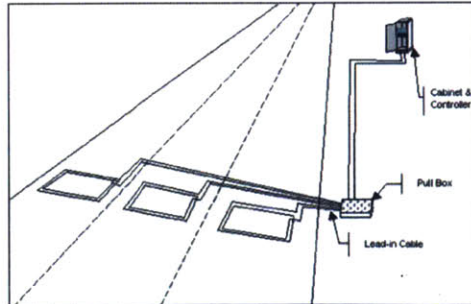


Figure 2.3: The loop detector used for road measurements.

The maximum value of the density downstream of the user’s entry point determines the toll price, and the entering driver is charged that value. The HOT toll price changes every three minutes and the HOT driver is charged automatically through a transponder that is leased from the MN Department of Transportation (MnDOT). HOV’s must also have a transponder to utilize free passage on the HOT lane. The toll price is determined based on the current traffic density and the change in density, as seen in the chart in Fig. 2.4. The success of MnPASS on I-394 and I-35 has been touted as a success, and there are current plans of expanding the dynamic pricing program to other roads in the Minneapolis area.

Table 2: Pricing Plan for Normal Operation of MnPASS Lanes (both I-35W and I-394)

Level of Service	Min K	Max K	Min Rate (\$)	Default Rate (\$)	Max Rate (\$)
A	0	11	0.25	0.25	0.50
B	12	18	0.50	0.50	1.50
C	19	31	1.50	1.50	2.50
D	32	42	2.50	3.00	3.50
E	43	49	3.50	5.00	5.00
F	50	50	5.00	8.00	8.00

Density in veh/mi/ln; Prices in \$

Table 3: Price Changes Based on Change in Density - Used for all pricing plans

Density	$\Delta 1$	$\Delta 2$	$\Delta 3$	$\Delta 4$	$\Delta 5$	$\Delta 6$
0-18	0.25	0.25	0.25	0.25	0.25	0.25
19+	0.25	0.50	0.75	1.00	1.25	1.50

Density in veh/mi/ln; Prices in \$

Figure 2.4: A table of the MnPASS pricing system. Here K represents the density. A default rate is chosen based what level of service the maximum density falls in and is adjusted based on the change in density. Minimum and maximum values o

2.3 Literature Review

2.3.1 Traffic Flow Theory

In addition to the economic viewpoint, the research of traffic congestion can be approached from a physics and transportation standpoint as well. An understanding of traffic flow physics is necessary in creating a successful dynamic toll pricing scheme since the toll price must react in real-time to the changing dynamics of the traffic flow. There are three categories of traffic flow models. Microscopic models analyze the dy-

namics of individual cars, macroscopic models view traffic as a continuum fluid, and mesoscopic models are formed by the combination of micro- and macroscopic models [23]. Microscopic models define the position, x_i and velocity, v_i , of every vehicle unit, i and are utilized by most of the traffic simulation programs available today. Examples of microscopic models include the Wiedemann model [15], Intelligent driver model [18], and the Nagel-Schreckenberg model [20].

Macroscopic models, on the other hand, equate traffic flow to a fluid stream and model the overall system of traffic flow. The groundbreaking research of Lighthill and Whitham [19], and Richards soon after [21], set the ground for traffic flow research. Lighthill and Whitham had conducted research on the behavior of rivers in floodplains and had extended their theories into the transportation field. Denoted as the Lighthill-Whitham-Richards (LWR) model [19,21], their traffic model is a kinematic model using a particle-flow analogy. The LWR model equates vehicles with particles and combines conservation of traffic flow equation with a traffic equilibrium model,

$$\frac{\partial q}{\partial t} + \frac{\partial \rho}{\partial x} = 0 \quad (2.4)$$

and

$$q(\rho, v) = q(\rho). \quad (2.5)$$

Together, these two equations form the LWR model. While equation (2.4) arises from the principle of conservation, equation (2.5) is an assumption made by the authors. In actuality, ρ and v are independent variables which, in turn, define the flow, $q = \rho v$. Because equation (2.4) is not enough to define a traffic stream equation (2.5) is necessary to find a solution. Equation(2.5) is often called an equilibrium equation as $v = v(\rho)$ occurs when the highway is sufficiently long and the traffic flow is in steady-state. The equilibrium equation is an empirical relationship found from traffic measurements and can take many forms (i.e. Greenshields' [13], Greenberg's [12]).

Within the last two decades, however, second-order models, such as the Aw-Rascle-Zhang (ARZ) model [6,29] have been extensively studied. These models employ two equations: the conservation of vehicles (2.4) and a momentum equation. The momentum equation is an empirical, partial differential equation that describes the acceleration and inertia of vehicles extended to a macroscopic scale, thereby providing a characterization of the traffic flow in non-equilibrium states. The advantage

of higher-order models over first-order models is that they are able to describe certain traffic phenomena observed that cannot arise from simpler models like the LWR model, for instance, hysteresis, density bifurcation, and stop-and-go traffic. Many authors have proposed different forms of momentum equations, (see references in [6]). While the LWR model has been analyzed and incorporated into many toll pricing studies, research on the integration of the ARZ model and toll pricing is lacking due to its complexity and difficulty in parameterization.

2.3.2 Dynamic Pricing Research

Notable contributions in the study of dynamic pricing have been that of Zhang [27], Janson [17], and Yin [26]. Zhang et al. incorporated the LWR model in their pricing strategy and conducted dynamic toll pricing simulations in the Seattle area in order to understand the differences an HOT and HOV lane had on alleviating congestion. Janson and Levinson at the University of Minnesota have conducted various, comprehensive studies on dynamic toll pricing in Minneapolis [17]. Coordinating with MnPASS policy-makers, they have tested different toll pricing schemes to better model driver elasticity and decision-making. Their approach to toll pricing differs by offering a discrete table of prices as their pricing controller, and is more empirical than Zhang's analytical method. The research they have conducted, however, is important in providing detailed driver behavior information on the MnPASS system, specifically. Yin and Lou compared two different tolling strategies, a traditional proportional feedback controller and a self-learning controller, to find the toll price that would optimize traffic throughput and provide a better travel service to drivers. Their methods were tested in simulation, and they found that the self-learning pricing scheme provided a better service, but at a higher cost and with greater implementation difficulties. The work in this thesis is most similar to Zhang's but incorporates information from Janson and Levinson to focus on the MnPASS system.

Chapter 3

Socio-Technical Model

For the work in this thesis, the underlying road geometry is assumed to consist of an HOT lane and a GPL in parallel (see Fig. 3.1) as this is the most common implementation. This entire road section will be referred to as a road segment throughout the thesis. A critical assumption is that there are no lane changes between the HOT and GPL lanes for the segment considered.

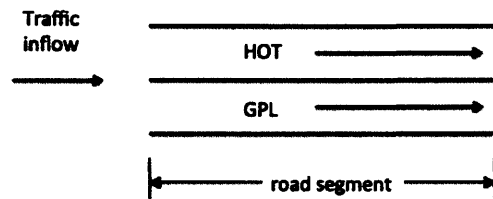


Figure 3.1: A physical schematic of the road segment. The HOT lane is in parallel with the GPL. No traffic flows between the two beyond the initial entry point.

The procedure used in this research to determine the overall controller begins with a desired density in the HOT lane. Any departure of the actual density from this value is fed into our price controller, which is the main component of our proposed approach. The resulting output of the controller is the toll price of the HOT lane, which enters as an input into the socio-technical model. The socio-technical model consists of the driver behavior model, which represents the driver's decision of whether or not to enter the HOT lane, the traffic flow model, which captures the dynamics between the incoming traffic flow and outgoing traffic density of the underlying road segment,

and the traffic equilibrium model, which gives the relationship between traffic density, flow, and speed. In the following sections, each of the components in this higher-level feedback loop, shown in Fig. 3.2, are explained in detail.

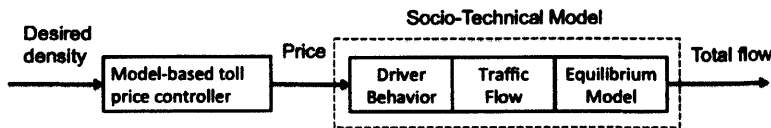


Figure 3.2: A higher-level block diagram for our dynamic pricing system. The price influences the number of drivers that go into each lane, which is determined by the driver behavior model. The number of vehicles, then, affect the lane densities, closing the loop.

3.1 Traffic Flow Model

3.1.1 Traffic Flow Dynamics

Incorporating a model for traffic flow is crucial in understanding the underlying dynamics and developing a pricing scheme to prevent the onset of congestion. As our focus is on the dynamics when the traffic is close to congestion where the traffic is in an unsteady state, we do not use the LWR model which focuses on steady characteristics of traffic flow. Instead, we use an accumulator model that is an aggregate, lumped parameter model that captures the most dominant dynamics. The density of the road segment is found by tracking the ingoing and outgoing vehicles in the segment. The incoming flow, $q_{in,HOT}$, is an input into the system, and the outgoing flow, $q_{out,HOT}$ is assumed to be a time delay of the incoming flow because of the relatively short length of the road segment. In actual implementation, the outgoing flow would also be an input from the road sensors. This time delay model is first order, whose time constant, τ , depends on the average speed, \bar{v} , of the traffic stream. Qualitatively, τ represents the time it takes a car to traverse a road segment of length L ,

$$\frac{q_{out,HOT}(s)}{q_{in,HOT}(s)} = \frac{1}{\tau s + 1} \quad (3.1)$$

where $\tau = L/\bar{v}$.

The average density, ρ is determined based on the current inflow (derived from real-time sensor measurements) with the following equation,

$$\rho(t) = \frac{\int_0^T q_{in}(t) - q_{out}(t) dt}{L} \quad (3.2)$$

With these, we can derive the underlying transfer function for the HOT lane as

$$\frac{\rho(s)}{q_{in}(s)} = \frac{\tau/L}{\tau s + 1} \quad (3.3)$$

A similar traffic model was assumed for the fixed toll lane as well.

In contrast to the MnPASS model, which evaluates local densities, our system calculates the average density, ρ , of the road between two sensors by tracking the vehicles that enter, $q_{in}(t)$, and exit, $q_{out}(t)$, the road segment. The number of cars that lie in the road segment is known based on the volume measurements from the loop detectors, and the length of the segment is a fixed value; therefore, ρ is known based on existing data, barring an offset of the initial number of cars in the segment. This accumulator method gives a better estimation of the road conditions inside the segment than the MnPASS system, where only local densities over the length of the field sensor are being measured.

3.1.2 Traffic Flow Dynamics Parameterization

In order to determine the traffic flow model, density and speed measurements were taken from the MnPASS system. A 0.7 mile road segment was chosen, $L = 0.7$, which in turn, gives us the value of the time delay,

$$\tau = \frac{0.7}{\bar{v}}. \quad (3.4)$$

The entry and exit points of this road segment are shown in Figure 3.3, marked as S77 and S37, respectively. Analysis of this road segment was ideal due to the lack of on- or off-ramps and the inability to switch between HOT and GPL lanes.

3.2 Traffic Equilibrium

3.2.1 Equilibrium Model and Parameterization

The price controller that we propose in this paper employs a reference density; the rationale behind this is that density is a direct metric of congestion and, in addition,

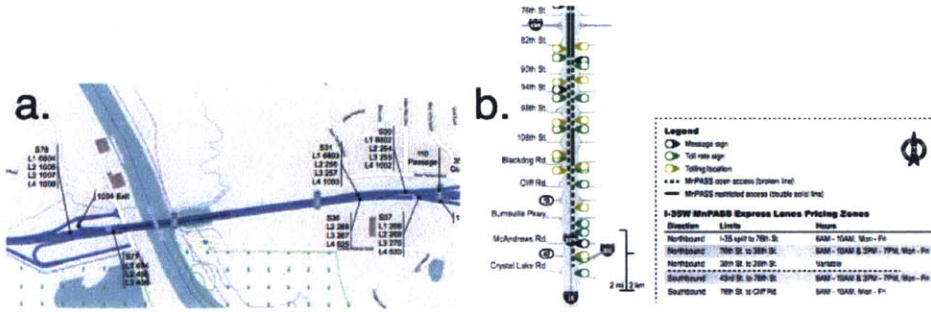


Figure 3.3: The physical map of the road segment (3.3a) and the schematic (3.3b). The road segment chosen lies on I-35W. Black dots on 3.3a indicate sensor locations. Figure 3.3b reveals operational details concerning the location of toll collection, restricted entrances, and toll rate signs.

provides a convenient tool for optimizing the proposed algorithm. The traffic flow model provides the output density from the input flow, but furthermore, we need to determine the lane velocities in real time. The relation between traffic density and speed for various traffic conditions is nonlinear and complex and discussed in Chapter 2.3.1. While in general, velocity decreases with density, the underlying gradient changes drastically depending on whether or not the density exceeds a critical threshold (see Fig. 3.4). Using this feature, we propose a simplified equilibrium model, similar to Greenshields', as

$$\bar{v}(\rho) = \begin{cases} v_{free-flow} & \rho < \rho_{critical} \\ a\rho + b & \rho_{critical} \leq \rho \leq \rho_{critical} \\ v_{jam} & \rho > \rho_{jam} \end{cases} \quad (3.5)$$

In actuality, v_{jam} is zero, but that value produces an error in our model because nonmoving vehicles would stop the simulation. To overcome that, v_{jam} was given a small value of 2 mph.

To find the parameters for the equilibrium equation, density and speed information from MnPASS for the year 2014 at S36 (Fig. 3.3) was collected and averaged over a five minute period to obtain the equilibrium data used in Fig. 3.4. Blank sensor readings and speeds over 100 mph were discarded for feasibility reasons.

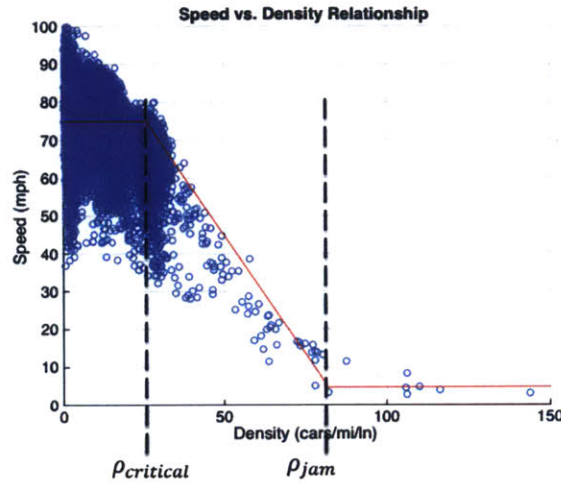


Figure 3.4: The equilibrium relationship between speed and density.

3.3 Alternative Traffic Models

It is recognized that the traffic equilibrium model is an empirical equation and, likely, a simplification of the actual traffic physics. Different traffic dynamic models were studied and put aside, due to either model complexity or difficulty in parameterizing the model to fit the MnPASS data provided. For the former reason, higher order traffic flow models were not used. A second-order model was not used for this research because of the inability to find a closed form solution to use in the feedback loop, in addition to the inability to parameterize the MnPASS system to fit the model.

Another traffic model that was studied, however, was a hysteresis traffic equilibrium model. Traffic hysteresis has been observed in [28], and a study of its theory was detailed in [28] as well. Instead of having an equilibrium equation in the form of Eq. 3.5, there would be a hysteresis loop in the congested region (see Fig. 3.5). The theory behind a traffic hysteresis loop is that traffic entering congestion can behave differently than that exiting congestion. Drivers entering congestion react to the increased density of traffic congestion, while drivers exiting congestion react to the increased speeds of the traffic flow. While hysteresis loops were observed in MnPASS data, the lack of consistency in the observed data made parameterizing a hysteresis

model difficult, and therefore, such a model was discarded in favor of 3.5.

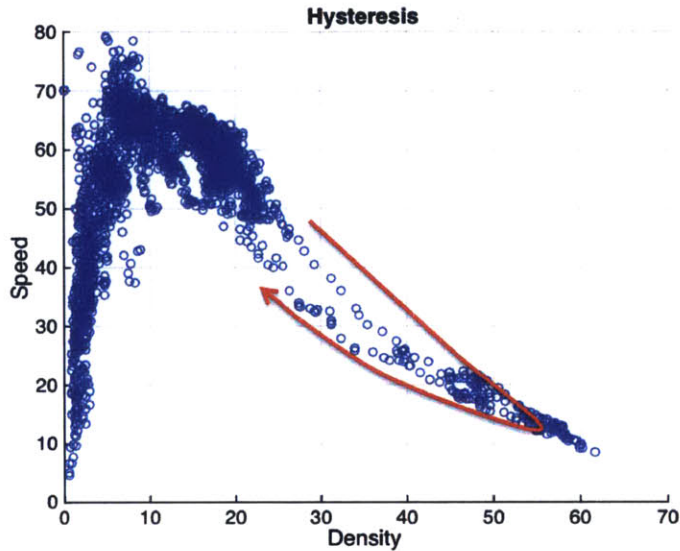


Figure 3.5: A hysteresis curve in the congested region of traffic.

3.4 Driver Behavior Model

Within the socio-technical model, there is the social aspect of the driver behavior and decision-making. Modeling driver behavior is vital in developing an effective pricing scheme. Since the goal of this system is to direct vehicles to desired lanes in certain quantities, understanding the motivations of drivers cannot be neglected.

3.4.1 Logit Model

Each individual driver entering the road segment has a discrete choice of entering the HOT or the GPL lane. The choice is essentially based on the lane that offers a higher utility U , and can be captured in a commonly used logistic model [7]. We choose the utility function to be a linear combination of the travel time T and toll price P , as

$$U = -\alpha T - \beta P + \gamma \quad (3.6)$$

where α and β represent the weighting of travel time and price, respectively, and γ is an offset term used to represent other unobservables (i.e. value of reliability in

choosing the HOT lane). As the goal is to minimize T and P , the negative signs in (3.6) allow the problem to be cast as the maximization of U . The negative signs result from the fact that travel time and tolls are undesirable to the driver.

The marginal utility ΔU of choosing the HOT lane vs. GPL lane can therefore be represented as

$$\Delta U = U_{HOT} - U_{GPL} = \alpha\Delta T - \beta P_{HOT} + \gamma \quad (3.7)$$

where ΔT represents the time savings of travel in the HOT over the GPL lane, and P_{HOT} denotes the price of the HOT lane (assuming the GPL lane has zero tolls). The time savings ΔT is determined by road segment length and the speed of the two lanes at the entry point,

$$\Delta T = L\left(\frac{1}{v_{GPL}} - \frac{1}{v_{HOT}}\right). \quad (3.8)$$

The assumption is that the drivers make an estimate of the road speeds and a corresponding ΔT .

It should be noted that the driver behavior model in 3.7 can be extended to a macroscopic scale. The driver's discrete choice to choose the HOT lane, when extended to model a population of drivers, smooths out and becomes a logistic model that describes the fraction of drivers that take the HOT lane, $\frac{q_{HOT}}{q_{in}}$. The aggregate driver behavior model is summarized below, and a visual of the logistic model is displayed in Fig. 3.6. The input from the driver behavior model then changes the input flow as

$$q_{in,HOT} = f(\Delta T, P_{HOT}) * q_{in} \quad (3.9)$$

where

$$f(\Delta T, P_{HOT}) = \frac{1}{1 + e^{\alpha\Delta T - \beta P_{HOT} + \gamma}}. \quad (3.10)$$

3.4.2 Driver Behavior Parameterization and Recursive Least Squares Estimation

In order to determine the parameters of the logistic driver behavior model, volume and speed data was taken from 6am to 10am, Monday to Friday, between November

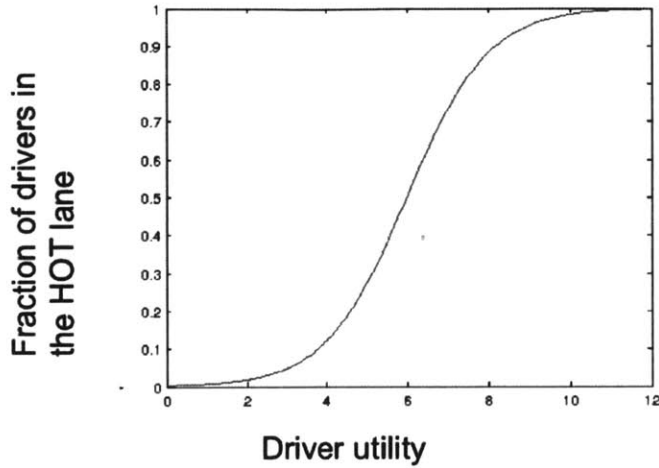


Figure 3.6: The logistic model used to characterize driver behavior and determine the HOT usage. The input to the model is the driver utility, which is a weighted sum of the current toll price and perceived time savings.

2013 and January 2014. Price data was obtained directly from MnPASS operators, and the driver volumes used were taken from the MnPASS program DataExtract. As the patterns seemed to vary significantly from one weekday to the next, a set of parameters, one set for each day, was determined.

Using MATLAB’s `glmfit` function (which uses Newton’s method to fit the data to the logistic model), the coefficients for the driver utility model, α , β , and γ were determined. Table 3.1 summarizes the results of the model fitting with the standard deviations shown in parentheses. A value of travel time savings metric, VOT, can be calculated from the coefficient values as

$$VOT = \left| \frac{\beta}{\alpha} \right| \quad (3.11)$$

which represents the amount per minute of time savings that the overall population of drivers is willing to pay. This value can also be used to determine the cost of traffic congestion, such as that mentioned in the introduction.

Comparison with recommended values by MnDOT (0.2667 \$/min) and USDOT (0.3817 \$/min) show that the values calculated in this study are close but consistently higher, with the exception of Thursday’s values [2, 5]. This pattern follows logically, since drivers opting for HOT lanes would naturally have higher values of travel time

savings, compared to the average values provided by MnDOT and USDOT. Improvements in the parameter fitting were seen when categorizing results by the day of the week. The values of γ show little variation between days and were, therefore, fixed at a constant value of -1.71781 for our model. Cases of severe congestion did occur in the sampled time, due to heavy snow and accidents. These days were not included in the analysis, as the congestion was significant enough to show degradation of the speed in the HOT lane equal to that of the GPL lanes.

Table 3.1: Mean values of fitted driver behavior parameters by day of the week

	Mon.	Tues.	Wed.	Thur.	Fri.	Average
α	-0.2879	-0.3409	-0.3953	-0.3710	-0.3026	-0.3340
β	0.3306	0.4182	0.3199	0.2936	0.3901	0.3550
VOT	1.148	1.227	0.8093	0.7915	1.289	1.063

Another key operational point is that of carpool users. In most current implementations of dynamic toll pricing in the U.S., vehicles with two or more passengers are authorized to use the HOT lane at no cost. MnPASS allows carpool vehicles the use of the HOT lane for free, and this consideration was taken into account, in both the parameterization of the data and the implementation of the simulation. With respect to the parameterization, a constant 55/45% split between carpool and paying users was assumed in the toll lane. More exact information can be gathered by obtaining the specific transponder log data from MnDOT; however, since little variation in carpool users is seen day to day, a constant percentage was chosen for this study. The driver behavior model in (3.9) is therefore changed as

$$q_{HOT} = 0.45 * f(\Delta T, P_{HOT}) * q_{in} \quad (3.12)$$

Chapter 4

Model-Based Price Control Strategy

With the overall socio-technical model determined as in Chapter 3 we now describe the model-based control strategy for the toll price in this section, the details of which are illustrated in Fig. 4.1. This controller consists of two parts, a linear dynamic component, and a nonlinear algebraic component. The former is a PD-controller, while the second is a logit function that serves as an inverse of the driver behavior model. In addition to these two parts, a feedforward component is added to the controller to add greater control authority. These are described in greater detail below.

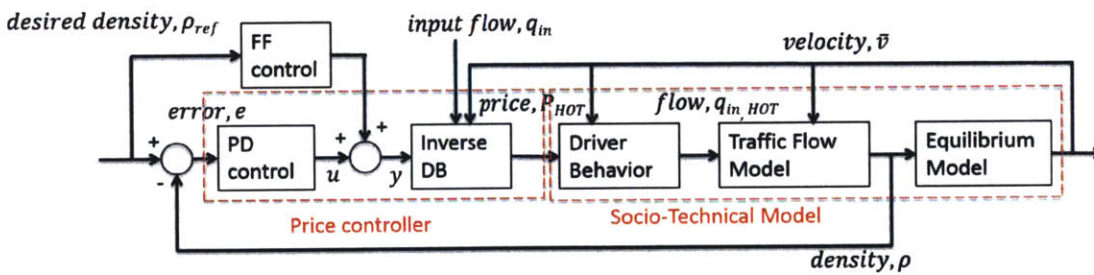


Figure 4.1: The inputs, subsystems, and variables of the entire system are shown in this representative block diagram. The input into the system is the desired density in the HOT lane, and the output is the actual density. The input flow is the measured, total flow into the system.

4.1 PD Controller

A PD controller is used to track the desired density relatively quickly and to prevent large increases in the HOT density:

$$u = K_p e + K_d \dot{e} \quad (4.1)$$

where the error $e = \rho_{ref} - \rho$, and K_p and K_d denote the proportional and derivative gains, respectively. The derivative component reacts to sudden changes in the system's density, thereby mitigating deviation from the traffic equilibrium model mentioned above. Moreover, the derivative (lead) term compensates the lag dynamics of the accumulator model of the road segment. An integral component was considered but discarded. The results later in this thesis show the PD controller tracking the target density without steady state error, and so an integral component to the price controller was not added.

4.2 Feedforward Controller

A feedforward component was added to the PD controller to provide greater control authority. Because the inverse driver behavior function is relatively flat near the lowest values of driver utility (see Fig. 3.6, a feed forward gain, $K_{ff} = a$ was added to ensure equilibrium when $\rho = \rho_{ref}$. The input, y , to the inverse driver behavior model is given by

$$y = K_p e + K_d \dot{e} + K_{ff} \rho_{ref}. \quad (4.2)$$

In addition, looking at Fig. 4.1, the input to the inverse driver behavior block is a value for flow, not density, so the feedforward gain also has the effect of translating the desired density into a desired HOT flow. That relationship follows from the equilibrium relationship (3.5) and the fact that $q = \rho v$. Hence the necessary feedforward gain is a .

4.3 Inverse Driver Behavior Component

Following the classical controller is the inverse driver behavior component. The purpose of the inverse driver behavior function is to compensate for the nonlinear behavior of the driver modeled as in Chapter 3.4. Ideally, this inverse function would yield a perfect cancellation with the driver behavior logistic function and reduce the system to a first order system with a variable time constant. This inverse function has two inputs: the total incoming flow, q_{in} , and y , which is akin to the desired flow into the HOT lane, and an output P_{HOT} , and is given by

$$P_{HOT} = \frac{1}{\beta} [\alpha \Delta T + \gamma - \ln(\frac{q_{in}}{y} - 1)] \quad (4.3)$$

4.4 Gain Tuning

Assuming that the inverse driver behavior model perfectly cancels out the nonlinearity, the underlying relationship between ρ_{ref} and ρ is a linear dynamic system of first-order with the transfer function,

$$\frac{\rho(s)}{\rho_{ref}(s)} = \frac{K_d s + (K_p + a)}{(K_d + L)s + (\frac{L}{\tau} + K_p)} \quad (4.4)$$

with a pole at

$$p = -\frac{(\frac{L}{\tau} + K_p)}{(K_d + L)}. \quad (4.5)$$

Therefore, one can use pole-placement methods to determine the PD gains. Since there is only one real pole, the system displays no overshoot. The PD gains were chosen such that settling time was approximately 3 minutes. Because the system pole depends on the velocity value, $\tau = L/\bar{v}$, a series of derivative gains were chosen for different velocities (see Table 2) with the proportional gain remaining constant at $K_p = 1.75$. The derivative gain was determined based on the settling time,

$$T_s = 4 * \frac{(K_d + L)}{(\frac{L}{\tau} + K_p)} = 3. \quad (4.6)$$

and so the corresponding derivative gain would be

$$K_d = \frac{3}{4}(\bar{v} + K_p) - L, \quad (4.7)$$

where L/τ was replaced with \bar{v} . The value for \bar{v} was chosen as the midpoint of the ranges in the first row of Table 2. This led to a selection of derivative gains,

Table 4.1: K_d values

$\bar{v} \in$	(0,15)	(15,30)	(30,45)	(45,60)	(60,75)
K_d	0.71	0.89	1.08	1.27	1.36

The feed forward gain, $K_{ff} = 0.43$ was chosen to corresponded the equilibrium model.

4.5 Results

The flow dynamics together with the driver behavior model are specified in Chapter 3, respectively. The parameters of this model are given by τ and α , β , and γ . The dynamic toll price strategy is specified in Chapter 4, along with the parameters of this strategy. We now describe the results obtained using out dynamic toll pricing controller in this chapter.

4.5.1 Model Validation

Our first step in validating the price controller proposed in Chapter 4 is the validation of the socio-technical model described in Chapter 3. As the MnPASS system has data available regarding P_{HOT} , $q_{in,HOT}$, $q_{out,HOT}$, and speeds, with their price controller determining the HOT lane price, we use their data for this validation (see Fig 4.2).

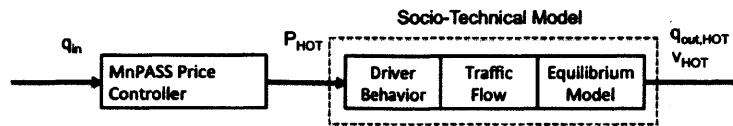


Figure 4.2: The MnPASS pricing controller was placed alongside our socio-technical model to validate the use of our system model.

The MnPASS price control algorithm is shown in Fig. 2.4. Because the MnPASS toll price is determined based on both the current density and the change in density

over time, a PD controller was chosen, without a feed-forward component or inverse driver behavior model, to recreate the MnPASS pricing system within our simulation environment. A variety of PD gains were tested in order to obtain results similar to the actual, measured data. The best match in results occurred when $K_p = 0.25$ and $K_d = 1.3$. The low proportional gain results from the lack of a target density in the MnPASS pricing scheme. A price cap was set at \$8 to reflect the MnPASS system. The resulting density and total flow obtained from MnPASS on Oct. 6, 2014 are shown in Figure 4.3 and compared with the estimated quantities using our socio-technical model given by Eqs. (3.3)-(3.12). Similar results were obtained for a range of dates in 2014. This result shows that our driver behavior model, traffic flow model, and equilibrium model is a reasonable approximation of the actual traffic flow.

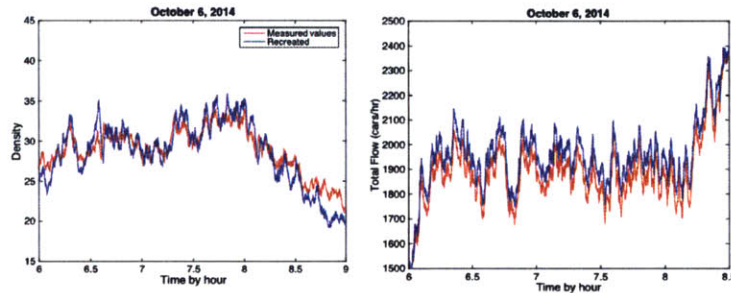


Figure 4.3: The similarity of the density and speed plots of our simulated system (blue) and the actual MnPASS system (red) validate the use of our model-based system.

4.5.2 Results of our Model-based Pricing Controller

We now use the socio-technical model in Chapter 3, with parameters $\alpha = -0.3026$, $\beta = 0.3901$, $\rho_{critical} = 25$, $\rho_{jam} = 80$, $v_{free-flow} = 65$, and $v_{jam} = 5$. With the inverse behavior model as in eq. (4.3), and the control gains chosen as $K_{ff} = 0.4$, $K_d = 0.45$ and $K_p = 1.75$ and a desired density of $\rho = 30$, the overall traffic-flow with the price controller was simulated. The resulting density is shown in Figure 4.3a.

In order to generate a more aggressive strategy that quickly returns the HOT densities to the desired value, the PD gains were changed to such that the settling time was 1.5 minutes. The resulting responses are shown in Figure 4.4b that illustrate the significant improvement of our pricing controller in comparison with that of MnPASS.

To better illustrate the performance of our controller, an input flow that introduced congestion in the middle of the operating period was chosen. The input flow profile has a large increase of incoming cars from 8:00 to 8:30am. The corresponding densities as well as price profiles, speeds, and total flows, both for our controller and the MnPASS controller, are shown in Figure 4.5. These plots especially show the significant improvement in the increase of total flow in comparison to MnPASS. While the prices are larger, we note that the price cap of \$8 set by MnPASS was not violated anywhere. All of these plots corresponded to a desired density of 30 cars/mi.

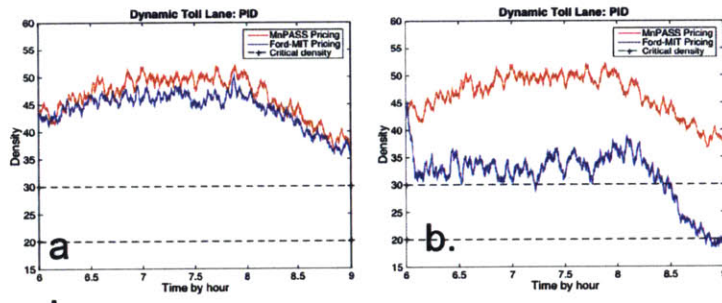


Figure 4.4: PID gains were chosen in 4.4a to match the behavior of MnPASS (red) and validate our system model (blue). The gains were changed for the simulation run in 4.4b to yield a more aggressive pricing scheme that was successful in preventing congestion in the HOT lane.

It is clear that instances of congestion still occur with the MnPASS pricing model, as their density climbs past the threshold between free-flow and congestion in 4 of the 5 graphs. Our pricing controller is targeting a density value near the critical density, so that the traffic flow remains in the linear, free-flow region. As a result, as is illustrated in Fig. reffig:congest, the corresponding densities remain below the critical density, despite the large input flow to the system.

Looking at the graphs of the toll prices, it is clear that the more aggressive PD gains are the key factor in preventing congestion. In addition, another strength of this pricing strategy is the ability to minimize flow and speed fluctuations, which is desirable for a better driver experience.

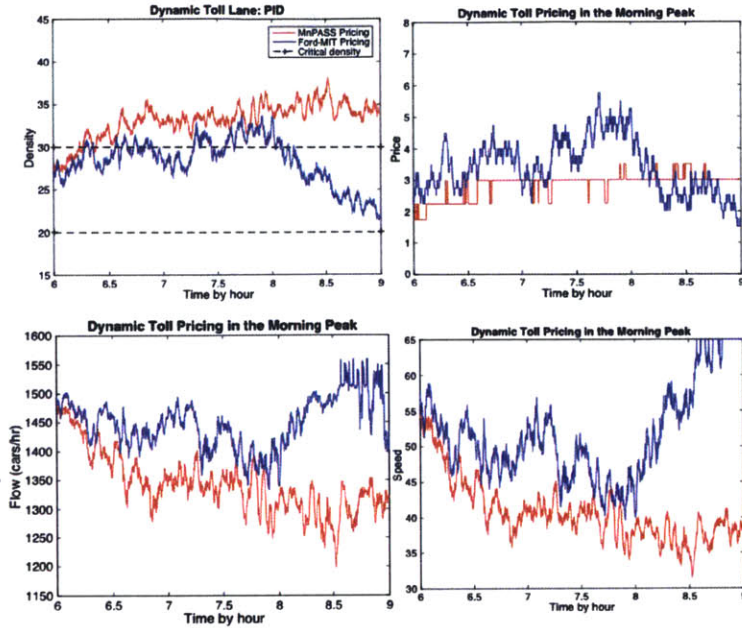


Figure 4.5: High input flow is introduced in the middle of the operating period to test the systems’ ability to prevent congestion. The model-based system is successful in keeping the HOT density low compared to MnPASS.

4.5.3 Effect of the Inverse Driver Behavior Component

Simulations were run without the inverse driver behavior component in the pricing scheme. Theoretically, this has the effect of introducing an unknown gain into the system. The results are shown in Figure 4.6, with and without the inverse function, and it can be seen that in the latter, the tracking error in density is much poorer when compared to the former.

We also evaluated the effect of an incorrect inverse driver behavior model. For this purpose, we replaced the parameters α and β by $\lambda_\alpha\alpha$ and $\lambda_\beta\beta$ respectively, with $\lambda_\alpha = 5$ and $\lambda_\beta = 2$. The resulting density response is shown in Figure 4.6 (in blue), and compared with the correct parameter values, i.e. $\lambda_\alpha = 1$ and $\lambda_\beta = 1$. As these plots show, the pricing control performance is somewhat insensitive to the inverse driver behavior parameters. But as Figure 4.6 shows, the pricing control performance is sensitive to the presence of the inverse nonlinearity itself.

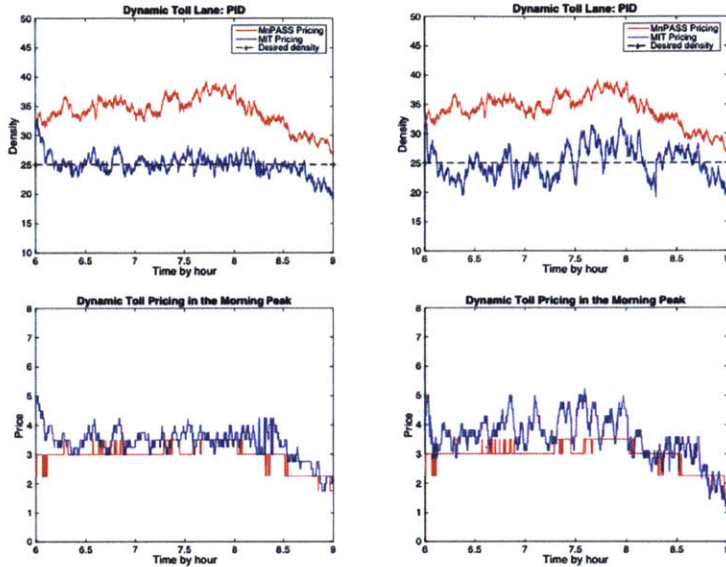


Figure 4.6: While the system without the inverse driver behavior pricing component (right) is able to keep the system from experience congestion, it fluctuates about the target density much more than the system with the inverse behavior component (left).

4.5.4 Target Density Selection

With Chapters 3 and Chapters 4 determining the traffic model parameters, the behavioral model parameters, and the PD control gains, the only quantity that remains to be determined is the desired traffic density, which is a reference signal into the whole closed-loop. The results above have target densities set to either 25 or 30, based on the value $\rho_{critical} = 30$. It is possible, however, that a strict value like that may not be optimal, especially in scenarios with high input flow. The target density should potentially adjust based on the overall traffic conditions.

Looking at the fundamental diagram, for a given input flow and desired HOT minimum speed, there are a variety of HOT and GPL densities that result. For a specific choice of those two variables, the overall output flow is maximized, and that operating point can be referred to as a sweet spot. At this point, the speed decrease to the GPL is minimal, the guarantees to the HOT users are satisfied, and the system benefit is achieved with the maximization of overall flow. Simulations run with constant input flows were conducted with different reference densities. These results are compiled in Fig. 4.7 and show that, with an increasing input flow, the target density should increase.

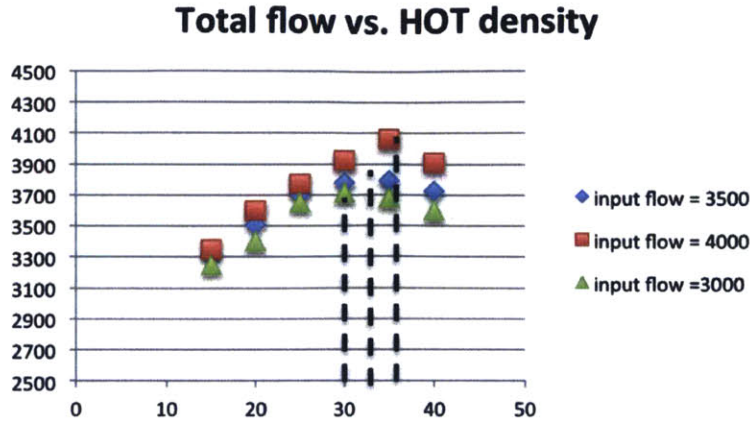


Figure 4.7: Increasing the reference density can increase the overall segment flow to maximize throughput.

4.5.5 Revenue Effects

An important component in any new toll pricing system is effect it will have on revenue generation. Because the proposed pricing strategy can be implemented within the existing infrastructure without any modifications to the infrastructure, any differences in revenue will result from the changes in toll prices and toll lane users. The revenue generation was calculated based on the number of HOT users and the toll price at the time of entrance into the road segment. Comparisons between the existing MnPASS system and our model-based system are displayed below (Fig. 4.8) for multiple days. The results indicate that the proposed model-based system results in the same or higher revenues for all cases. This could certainly change if the controller gains are chosen to be less aggressive, but again, that is a design choice that can be easily altered.

4.5.6 MATSIM

In addition to simulation in MATLAB, traffic simulations were conducted in a program called Multi-Agent Transport Simulation (MATSIM). MATSIM is a microscopic traffic environment that simulates the movement of individual vehicles to determine the traffic flow, density, and speed. The simulator was developed by researchers at ETH Zurich and is based on the traffic model in [20]. To further test the validity of

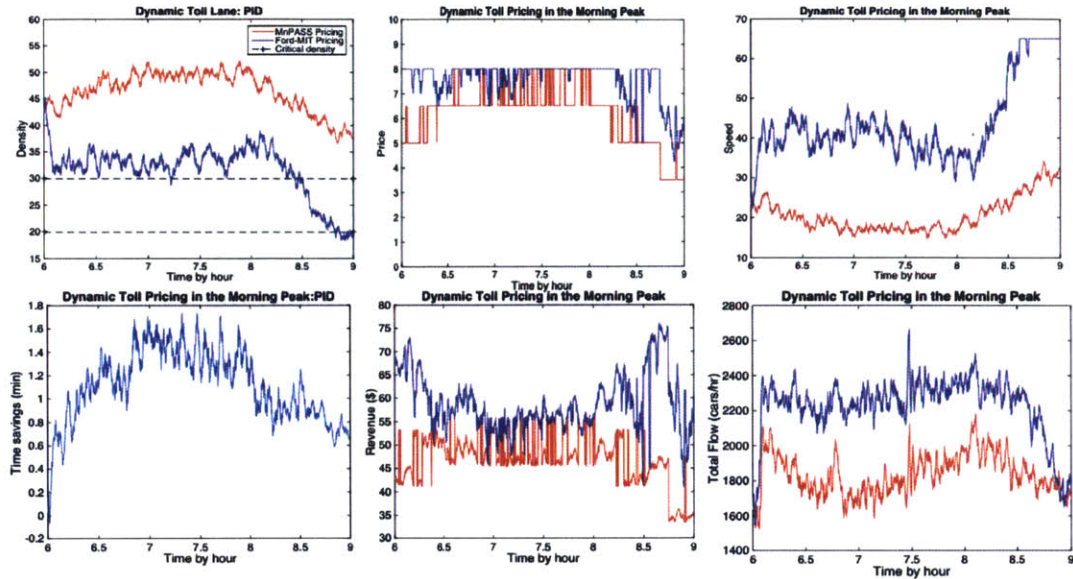


Figure 4.8: With an aggressive choice for the pricing controller, revenue can increase while maintaining the speed advantage in the HOT lane.

our socio-technical model and results, our model-based pricing scheme was inserted into MATSIM (see Fig. 4.9). Effectively, their microscopic traffic model replaced our traffic flow and equilibrium model, described in Chapter 3.



Figure 4.9: Testing our pricing controller in MATSIM.

The results comparing the performance of our pricing scheme in MATLAB and MATSIM are shown in Fig. 4.10. The similarity in the two density profiles shows that our traffic flow and equilibrium model hold up when compared to microscopic traffic flow models.

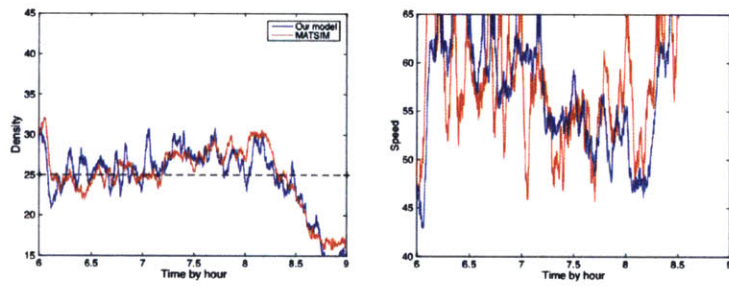


Figure 4.10: Testing our pricing controller in MATSIM.

Chapter 5

Conclusion and Future Work

5.1 Contributions of this Thesis

A real-time dynamic toll pricing scheme has the capability of reducing traffic congestion without the significant infrastructure costs that other alternatives, such as road expansion and public transportation development, require. In this thesis, a model-based dynamic toll-pricing strategy was proposed based on a socio-technical model, which was verified using real data and simulation.

Based on measured values from the MnPASS network, the socio-technical model was validated. The toll-pricing strategy consisted of a nonlinearity that served as the inverse driver behavior model, and a simple PD controller. Using data from the actual traffic inflow from MnPASS and simulations of our socio-technical model and the dynamic pricing controller, the results of our toll pricing controller were obtained, and shown to successfully reduce traffic congestion more effectively than the current MnPASS pricing scheme.

Of late, the concept of the Smart City is gaining popular attention, driven by goals of sustainability and efficiency, the needs of enhancing quality and performance, and the explosion of technological advances in communication and computation [22]. Given that 50% of the world's population lives in urban regions, critical infrastructures of transportation, energy, healthcare, and food as well as their growing interdependencies have to be collectively analyzed and designed to provide the substrate for the realization of the Smart City Concept. The dynamic toll pricing scheme proposed in this thesis can be viewed as one of the foundational blocks towards the realization of Smart City.

5.2 Discussion of Future Work

Several areas of study remain in this line of work. Extensions to highway systems with more lanes, merges, and entry and exit ramps, will all require more precise modeling and analysis. The role of more complex behavioral models as well as nonlinear and distributed traffic flow models can be carefully examined as well. Impact of carpool drivers and other nonlinear effects such as hysteresis in severely congested flows remain to be investigated. In addition, further development in MATSIM can provide quicker analysis and research of effective pricing strategies, which could also be of use to transportation authorities and officials. Also, the implementation of dynamic pricing has occurred in many other cities and this research could be extended to those systems as well.

The work of this thesis analyzes congestion management from the side of the transportation authorities, but there is also Smart City work being done from the position of the individual drivers wanting to limit the traffic congestion they experience. This thesis can be extended beyond management of highway traffic into management of city traffic from the perspective of individual drivers and private businesses with the results and methods in [11].

Bibliography

- [1] 495 — 95 Express Lanes - Pricing.
- [2] Benefit-Cost Analysis for Transportation Projects.
- [3] I-85 Toll Rate Pricing.
- [4] Metro ExpressLanes.
- [5] USDOT VOT Guidance 2014.
- [6] A Aw and M Rasche. Resurrection of “Second Order” Models of Traffic Flow. *SIAM J. Appl. Math.*, 60(3):916–938, 2000.
- [7] M Ben-Akiva and Michel Bierlaire. DISCRETE CHOICE METHODS THEIR APPLICATIONS TO SHORT TERM TRAVEL DECISIONS. *Handbook of transportation science*, (1985), 1999.
- [8] Inc. Cambridge Systematics. I-394 MnPASS Technical Evaluation. Technical report, 2006.
- [9] David Schrank, Bill Eisele, and Tim Lomax. 2012 Urban Mobility Report. Technical report, 2012.
- [10] Mark Goh. Congestion management and electronic road pricing in Singapore. *Journal of Transport Geography*, 10(1):29–38, 2002.
- [11] Marta C González, César A Hidalgo, and Albert-László Barabási. Understanding individual human mobility patterns. *Nature*, 453(7196):779–782, 2008.
- [12] H. Greenberg. An Analysis of Traffic Flow, 1959.

- [13] B.D. Greenshields, JR Bibbins, WS Channing, and HH Miller. A study of traffic capacity. In *Highway Research Board Proceedings*, pages 448–477, 1935.
- [14] Kalman Gyimesi, Charles Vincent, and Naveen Lamba. Frustration Rising : IBM 2011 Commuter Pain Survey. Technical report, 2011.
- [15] Bryan Higgs, MM Abbas, and Alejandra Medina. Analysis of the Wiedemann Car Following Model over Different Speeds using Naturalistic Data. *3rd International Conference on . . .*, pages 1–22, 2011.
- [16] IBM. Building a smarter transportation management network - LBW03019USEN.PDF, 2014.
- [17] Michael Janson and David Levinson. HOT or not driver elasticity to price on the MnPASS HOT lanes. *Research in Transportation Economics*, 44(1):21–32, 2014.
- [18] Arne Kesting, Martin Treiber, and Dirk Helbing. Enhanced intelligent driver model to access the impact of driving strategies on traffic capacity. *Philosophical transactions. Series A, Mathematical, physical, and engineering sciences*, 368(1928):4585–4605, 2010.
- [19] M. J. Lighthill and G. B. Whitham. On Kinematic Waves. II. A Theory of Traffic Flow on Long Crowded Roads, 1955.
- [20] Kai Nagel and Michael Schreckenberg. A cellular automaton model for freeway traffic, 1992.
- [21] P. I. Richards. Shock Waves on the Highway, 1956.
- [22] R. Sengupta, A.M. Annaswamy, S. Amin, S. Moura, and V. Bulusu. Smart Cities and Control. *IEEE Control Systems Magazine (to appear)*, 2015.
- [23] U.S. Federal Highway Administration. Economics: Pricing, Demand and Economic Efficiency. Technical report.
- [24] William Vickrey. Pricing in Urban and Suburban Transport. *The American Economic Review*, 52(2):14, 1963.

- [25] Washington State Department of Transportation. SR 520 Toll Operations and Traffic Performance Summary Report 2012. Technical report, 2012.
- [26] Yafeng Yin and Yingyan Lou. Dynamic Tolling Strategies for Managed Lanes, 2009.
- [27] Guohui Zhang, Xiaolei Ma, and Yinhai Wang. Self-adaptive tolling strategy for enhanced high-occupancy toll lane operations. *IEEE Transactions on Intelligent Transportation Systems*, 15(1):306–317, 2014.
- [28] H. M. Zhang and T. Kim. A car-following theory for multiphase vehicular traffic flow. *Transportation Research Part B: Methodological*, 39(5):385–399, 2005.
- [29] H.M. Zhang. A non-equilibrium traffic model devoid of gas-like behavior. *Transportation Research Part B: Methodological*, 36(3):275–290, March 2002.

Appendix A

MATLAB/Simulink

This appendix provides the technical details on the simulations in this thesis. Raw MnPASS sensor data can be obtained from DataExtract or by contacting MnPASS officials.

A.1 Parameterization

To determine the traffic equilibrium relationship, density and speed measurements were obtained, separated into regions, and a linear regression was performed in the congested region.

```
% equilibrium equation parameterization
% enter density data into d and speed data into s

% average over 5 minutes
for t=11:(numel(d)-10)
    aved(t-10)=mean(d((t-10):(t+10)));
    aves(t-10)=mean(s((t-10):(t+10)));
end

ff_s=[]; % freeflow speed
cong_s=[]; % congested speed
jam_s=[]; % jam speed

% likewise for density
ff_d=[];
```

```

cong_d=[];
jam_d=[];

% define density parameters
dcritical=25;
djam=80;

% sort data into regions
for t=1:numel(aved)

    % eliminate negative speeds
    if aves(t)<0
        aves(t)=aves(t-1);
        aved(t)=aved(t-1);
    end

    % eliminate high speeds
    if aves(t)>=100
        aves(t)=aves(t-1);
        aved(t)=aved(t-1);
    end

    if aved(t)<dcritical
        ff_s(end+1)=aves(t);
        ff_d(end+1)=aved(t);
    else
        if aved(t)<=djam
            cong_s(end+1)=aves(t);
            cong_d(end+1)=aved(t);

            else
                jam_s(end+1)=aves(t);
                jam_d(end+1)=aved(t);
            end
        end
    end

end

v_freeflow=mean(ff_s);
v_jam=mean(jam_s);

```

```
p=polyfit(cong_d, cong_s, 1);
% linear relationship parameters in p
```

To determine the driver behavior parameterization, price data was obtained directly from MnPASS officials and volume and velocity data was taken from DataExtract.

```
% logistic model fit for each day in a month
% enter GPL speeds in s and HOT speeds in stoll

for i=1:480
    for j=1:31

        % eliminate negative speeds
        if s(i,j)<=0
            s(i,j)=s(i-1,j);
        end

        if stoll(i,j)<=0
            stoll(i,j)=stoll(i-1,j);
        end
    end
end

% volsum is the total volumn considered
% vol is the volumn of drivers entering the GPL
% voldyn is the volumn of entering the HOT lane
volsum=vol(:,1:31)+voldyn;

% price data, p
p=reshape(p,480,31);

% voldyn is multiplied by a factor of 0.45 to account for only the paying
% HOT drivers
volpaying=.45*voldyn;

% fraction in HOT lane by paying
y=volpaying./volsum;
```

```

% driver behavior parameters in B with std dev values in dev
B=zeros(4,31);
dev=zeros(1,31);

% time savings in delT
delT=1./s-1./stoll;

% eliminate negative time savings
for i=1:480
    for j=1:31

        if delT(i,j)<0
            delT(i,j)=0;
        end

    end
end

for k=1:31

    x=[delT(:,k) p(:,k) ones(480,1)];
    yfit=y(:,k);
    [B(:,k), dev(:,k)]=glmfit(x,yfit,'binomial','link','logit');

end

```

A.2 Simulink

The MATLAB simulations were conducted using the following Simulink. Input flow data can be obtained by extracting flow data from the preceding road segment in DataExtract or can be defined by the user.

